NOTES AND CORRESPONDENCE

A Green Planet versus a Desert World: Estimating the Effect of Vegetation Extremes on the Atmosphere

Klaus Fraedrich, Axel Kleidon, and Frank Lunkeit

Meteorologisches Institut, Universität Hamburg, Hamburg, Germany

ABSTRACT

The effect of vegetation extremes on the general circulation is estimated by two atmospheric GCM simulations using global desert and forest boundary conditions over land. The difference between the climates of a ''green planet'' and a ''desert world'' is dominated by the changes of the hydrological cycle, which is intensified substantially. Enhanced evapotranspiration over land reduces the near-surface temperatures; enhanced precipitation leads to a warmer mid- and upper troposphere extending from the subtropics (induced by ITCZ, monsoon, and Hadley cell dynamics) to the midlatitudes (over the cyclogenesis area of Northern Hemisphere storm tracks). These regional changes of the surface water and energy balances, and of the atmospheric circulation, have potential impact on the ocean and the atmospheric greenhouse.

1. Introduction

Land surfaces are distinctively different from oceans in that many properties and processes at their surface that are relevant to the atmosphere are controlled by the biosphere. Only in the presence of vegetation with sufficiently large access to soil moisture may a land surface appear like an ocean in terms of its energy balance and its evaporative behavior, if conditions are optimal for vegetation, that is, no deficiency of nitrogen, etc. The extent to which these parameters matter to the atmosphere and the water cycle has been demonstrated by sensitivity studies with atmospheric models at a variety of different scales (see the recent review by Pielke et al. 1998). So far, however, these sensitivity studies have been focusing either on regional aspects like Amazonian deforestation (e.g., Henderson-Sellers et al. 1993), on isolated parameters like albedo (e.g., Charney 1975), or on processes like land surface evapotranspiration (Shukla and Mintz 1982). But, from a biospheric viewpoint, these parameters and processes merely represent different aspects of vegetation and are dependent upon each other. For instance, vegetation will not stay green and keep a low albedo if sufficient soil water is not available.

Our approach here is to describe the control of the biosphere on land surface characteristics by one dimension, ranging from ''no vegetation'' to ''maximum vegetation.'' This approach is then used to assess the effect of these vegetation extremes on the atmosphere and its circulation. The maximum possible range is quantified by comparing two climate model experiments conducted at these extremes, the ''desert world'' extreme, in the absence of any vegetation, and the ''green planet'' extreme, with maximum vegetation. These extremes are chosen because they are characterized by the largest changes of parameters effecting the atmosphere. While these extremes may not be ecologically sustainable in a natural world, that is, representing equilibrium states of the climate biosphere system (e.g., Claussen 1998; Foley et al. 1998; deNoblet et al. 1996), we justify the use of these extremes by the human domination of the earth's ecosystems (Vitousek et al. 1997).

For the model experiments we utilize a state-of-the-art atmospheric general circulation model (GCM). The outline of this note is as follows. Section 2 describes the experimental design, the results are presented in section 3, and the discussion (section 4) hints at implications for the ocean heat flux and the atmospheric greenhouse.

2. Experimental design

The Hamburg climate model ECHAM4 (Roeckner et al. 1996) in T42 resolution (corresponding to 2.8° ×

Corresponding author address: Klaus Fraedrich, Meteorologisches Institut, Universität Hamburg, Bundesstr. 55, D-20146 Hamburg, Germany.
E-mail: fraedrich@dkrz.de

2.8°) is the basis for the numerical experiments. The model simulates the present-day climate realistically as described by the control simulations compared with observations (Wild et al. 1996; Roeckner et al. 1996; Stendel and Roeckner 1998). The Atmospheric Model Intercomparison Project comparison has rendered an ECHAM performance, in particular its hydrological cycle, in very good agreement with observations (Lau et al. 1996). Therefore, it is an ideal tool to determine the atmospheric general circulation at its extreme vegetation bounds.

Vegetation setting

An integral part of the model is the land parameterization scheme. It describes the interaction between the GCM's weather and soil by the surface fluxes of heat, water, and momentum. Soil hydrology is incorporated by a budget equation. It includes surface runoff (Dümenil and Todini 1992) accounting for the subgrid-scale terrain height inhomogeneities, the slow and fast drainage depending on the water content of the rooting zone, and the total evapotranspiration, which is composed of evaporation from snow, bare soil, transpiration, and reevaporation of water intercepted by the canopy. Accordingly, the land surface processes of the GCM that are associated with changes in vegetation are characterized by the following parameters: (a) albedo, (b) forest ratio, (c) vegetation cover, (d) leaf area index, (e) roughness length, and (f) soil water storage capacity. The standard set of land surface parameters and its derivation from observations is described by Claussen et al. (1994). Global desert and global forest conditions require changes of the land parameters, which, for our experiments, are prescribed as follows.

Desert world: the land surface parameters are set to desert conditions. (a) The albedo is 28% or larger, if it is exceeded by the standard background albedo; (b) the forest ratio and (c) the vegetation cover are set to zero; (d) the leaf area index is zero; (e) the roughness length attains the orographic values; and (f) the soil depth is taken as 0.1 m; conversion to soil water storage capacity is obtained by using soil texture information (Batjes 1996).

Green planet: the land surface parameters are set to forest conditions. (a) The albedo set to 12%; (b) the forest ratio and (c) the vegetation cover are 100%; (d) the leaf area index is 10, (e) the roughness length of vegetation is defined by 2 m; and (f) the soil water storage capacity is obtained by an optimization approach (Kleidon and Heimann 1998a) resulting in values that are sufficiently large to guarantee maximum soil water being available during dry periods. In addition, soil drainage is not possible and surface runoff occurs only when the rooting zone of the soil is at field capacity. Thus vegetation holds water in the soil at maximum capability, for example, by deep roots and high infil-tration due to high organic content and macropores of the soil.

3. Green planet versus desert world: Experimental results

The two experiments are run for a decade discarding the first year to avoid spinup effects. Sea surface temperatures and sea ice distributions are prescribed by the present-day climatological annual cycles to exclude oceanic feedbacks. Glacier areas over land are specified by an identical mask in both runs. Seasonal averages are shown for the Northern Hemisphere (NH) summer (June–August, JJA) and winter (December–February, DJF). In the figures presented, the desert world fields are taken as the reference while the differences green planet minus desert world illustrate the effect induced by the extreme of a green planet. The results discussed in this section concentrate on the global energy and water balance, and the dominant atmospheric circulation patterns.

a. Global water and energy balances

Comparing the global time mean water and energy budget (Figs. 1a,b) of the green planet and desert world shows the following highlights. The water cycle intensifies considerably. Over the continents evapotranspiration (E) triples and precipitation (P) doubles, while runoff is reduced by almost 25%. In addition, the precipitable water content over land increases by 31%. The enhanced land evapotranspiration is almost completely rained out over the continents. Compared with these magnitudes, the relatively small changes of solar radiative and sensible heat fluxes at the surface are expected to have a comparatively smaller impact: there is only less than a 5% increase in the net solar radiation. But the 67% reduction of the upward sensible heat transfer and a 30% decrease of the net upward thermal radiation make up for the observed tripling of the latent heat flux and the subsequent precipitation. That is, the water budget modification has the most substantial impact on the general circulation changes between the green planet and the desert world. These results are in agreement with a soil moisture–rainfall feedback mechanism proposed by Eltahir (1998; see also Delworth and Manabe 1988, 1989).

The atmosphere's response appears to be dominated by the enhanced water cycle, whereas changes in the net incoming solar radiation and surface albedo are less important. The surface albedo decrease is mostly balanced by an increase of the cloud albedo. Sensitivity experiments with changing albedo in the context of Amazonian deforestation confirm this effect (keeping the larger bucket size; Kleidon and Heimann 1998b). The green planet has a larger soil water availability due to the enhanced bucket size storing water for plant evapotranspiration in dryer seasons. More evapotranspiration

a

	atmosphere		
26		16	
27		21	
+4%		+31%	

421	464	71	31
410	443	137	108
-3%	-5%	+93%	+248%

ocean   37   **land**
                   28
                   -24%

b

100.0	38.9	68.2	
100.0	36.0	66.3	
0%	-8%	-3%	

atmosphere

55.6	18.9	111.1	89.3		
46.6	8.6	106.9	91.6		
-16%	-55%	-4%	+3%		

36.7	21.9	**land**	6.6	5.2
37.9	15.3		2.2	18.0
+3%	-30%		-67%	+248%

shortwave radiation	longwave radiation	sensible heat flux	latent heat flux
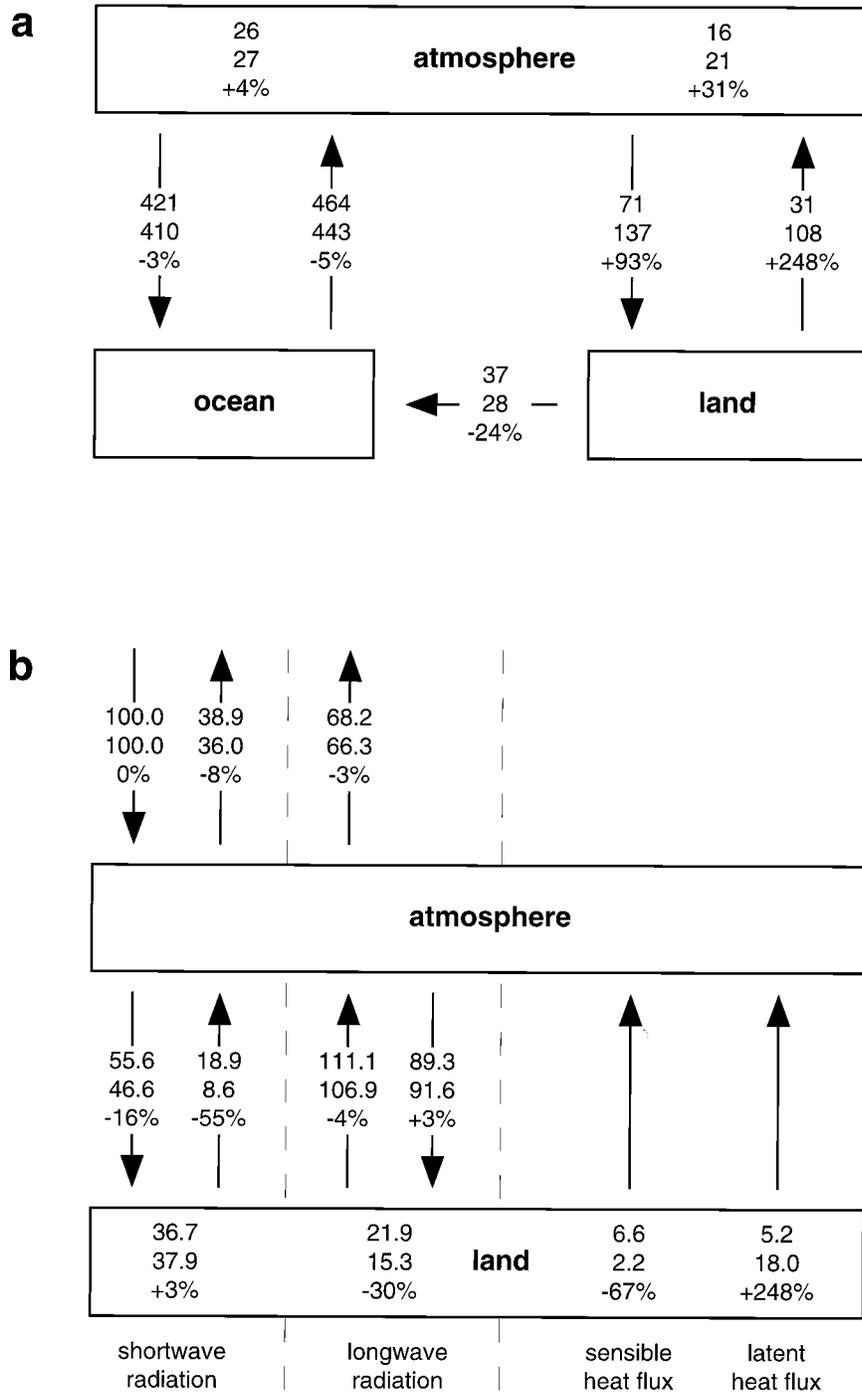
FIG. 1. Annual means of (a) the global water cycle and (b) the surface energy balance over land; annual mean water fluxes in 10^{12} m^3 yr^{-1}, precipitable water in kg m^{-2}, and heat/radiative fluxes in percent incoming radiation (100% = 341.3 W m^{-2}) of the desert world (upper), green planet (middle), and green planet minus desert world in percent (lower numbers).

leads to a reduction of the near-surface 2-m temperature over land by about 1.2 K. Increasing roughness length might also contribute to enhance the land surface exchange (e.g., Sud et al. 1988).

The related changes in the temperature field and the gross dynamical features of the general circulation can be directly inferred, that is, a warmer mid- and upper troposphere due to enhanced precipitation and a slightly
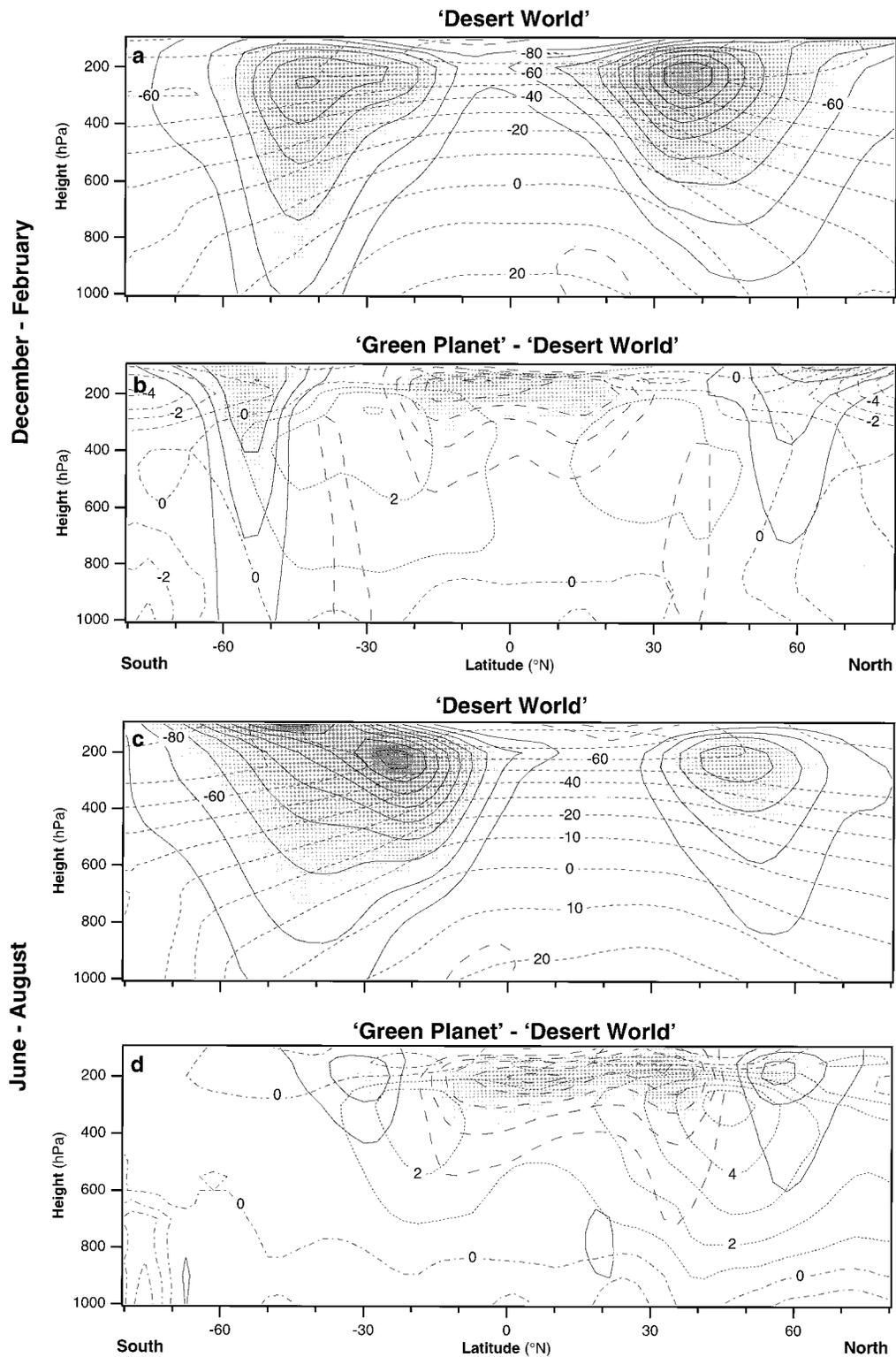
FIG. 2. Zonal means for [(a), (b)] DJF and [(c), (d)] JJA of air temperature (dotted contours denote positive values, dot-dashed negative values) and zonal wind (solid contours denote positive values, dashed negative values). Shown is the mean state of the desert world [(a): DJF, (c): JJA] and the differences between the green planet and the desert world [(b): DJF, (d): JJA]. Contour intervals for the mean states (differences) are 10 K (1 K) for air temperature and 10 m s^{-1} (2 m s^{-1}) for wind, respectively. Magnitude of wind is shaded gray. Numbers describe temperature contours in °C. Zero wind contours are omitted.

'Desert World'　　　　　　　　**'Green Planet'**
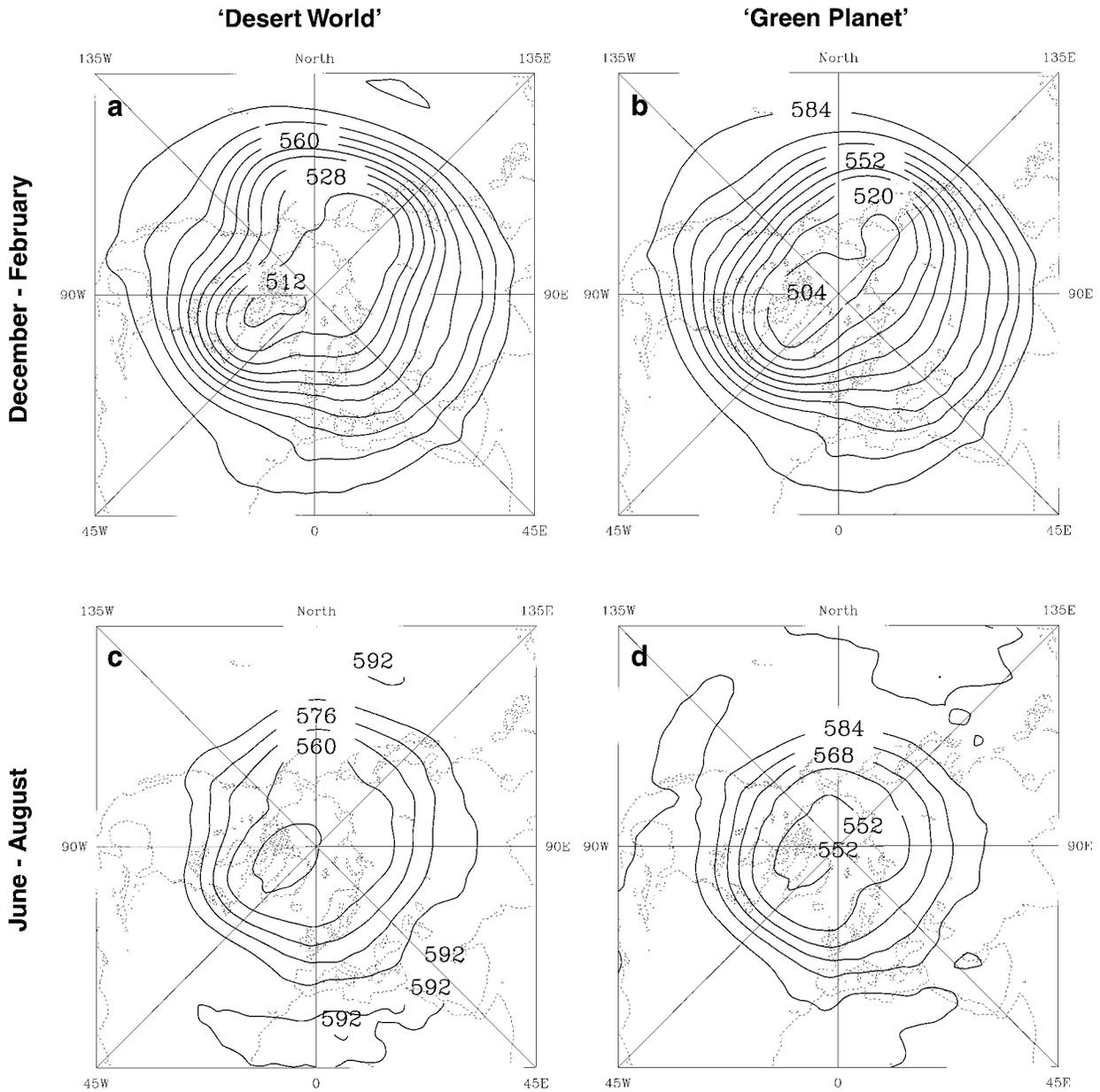
FIG. 3. Northern Hemisphere mean geopotential height (in gpdam; contours every 8 gpdam) and bandpass-filtered geopotential height variances (shaded) for DJF [(a), (b); different shading for 30, 40 and 50 gpm] and JJA [(c), (d); different shading for 10, 20 and 30 gpm] of the desert world [(a), (c)] and the green planet [(b), (d)].

reduced near-surface temperature due to the decreased sensible heat flux and boundary layer warming. This is a consequence of the enhanced evapotranspiration similar to the more locally confined oasis effect. The rainfall surplus and the reduced runoff add to the soil water available for evapotranspiration during the dryer periods. Thus largest changes can be expected over the NH in summer and during tropical dry seasons. Further details related to the large-scale structure of the general circulation will be discussed in the following section.

b. Atmospheric circulation patterns

The zonal mean seasonal temperature and wind distributions (Fig. 2) provide a first impression of the green planet and desert world circulation differences. These latitude–height cross sections are completed by the conventional 500-hPa maps of the time mean and the bandpass-filtered geopotential heights variance (Fig. 3) representing the mid- and upper-tropospheric dynamics (i.e., jet and stormtrack) in the NH. This is comple-
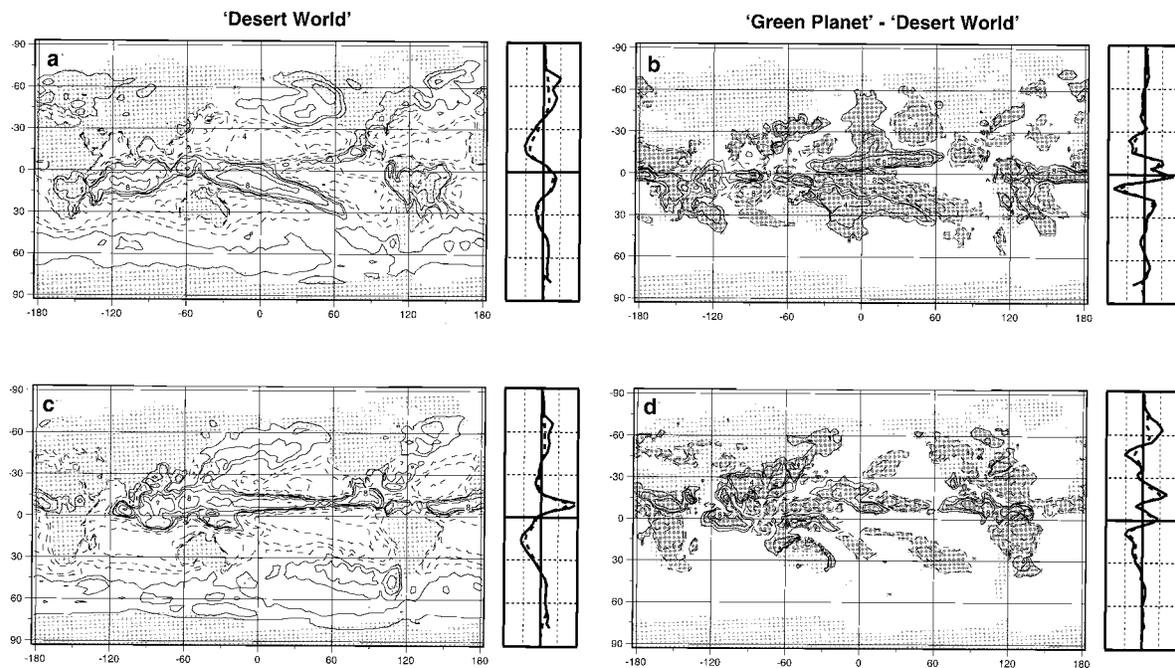
FIG. 4. Seasonal mean moisture flux (precipitation − evapotranspiration) in the desert world simulation for (a) DJF and (c) JJA and differences between the green planet and desert world climates [(b): DJF; (d): JJA]. Contours are at 1, 2, 4, 8, 16 mm day^{-1}. Negative values (dashed contours) mean net moisture flux into the atmosphere. Significant differences larger than 1 mm day^{-1} are shown in dark gray (Student's t-test, ≤0.05). Zero line contours are omitted. Light gray areas indicate land regions in which no significant changes take place. Right panels show zonal averages taken over the ocean (solid) and the full latitudinal band (dashed). Maximum values in zonal figures are 8 mm day^{-1} for (a), (c) and 2 mm day^{-1} for (b), (d).

mented by divergence of the vertically integrated mean moisture transport $(P - E)$ characterizing the lower-tropospheric flow and the water budget (Fig. 4; the zonal averages are plotted on the right panels). The following points are noted.

1) The mid- and upper-tropospheric temperatures are considerably higher in the green world case. The largest warming occurs in about 30° wide latitude belts in both the NH and the Southern Hemisphere (SH): In NH winter, their positions are symmetric about the equator near 30°N and 30°S with an indication of primary and secondary maxima north and south of 30°, respectively. In NH summer, both regions shift northward. Noteworthy is the enhanced response over the summer hemispheres, which is particularly strong (~4 K) in the NH and related to its dominating landmasses.

2) The position and strength of the jet streams and storm tracks change accordingly. They are displayed in Fig. 3 showing the seasonally averaged geopotential height fields and their bandpass filtered (2–6 days; Blackmon 1976) standard deviations for the NH. Compared to the desert world conditions, the summer and winter green planet storm tracks of the North Atlantic and North Pacific intensify substantially by enhanced latent heat release and extend downstream into the continents. As a consequence, the stationary

troughs and ridges are less pronounced, yielding a more zonally oriented circulation. The SH shows an almost closed circumpolar belt of high bandpass-filtered standard deviations that comes close to the conditions of an aquaplanet (not shown). As a consequence of the enhanced midlatitude zonality of the green planet, the Aleutian and Iceland lows are less intense. Compared to the global desert, this increases (decreases) the temperatures over the southeastern (northwestern) parts of the continents with more (less) moisture.

3) The intensification of the water cycle is observed everywhere with changes of both precipitation P and evapotranspiration E, balancing each other in many areas. However, regional water budget changes, $\Delta(P - E)$, may occur in the Tropics and subtropics, and in the midlatitudes (Fig. 4); the summer monsoon is enhanced in both hemispheres, $\Delta(P - E) > 0$, as well as the ITCZ. This is due to the continental moisture supplied by the increased evapotranspiration from the adjacent areas where $\Delta(P - E) < 0$, that is, the larger amount of precipitable water enhancing the lower-tropospheric moisture convergence into the convective systems. In the midlatitudes, downstream of the continental landmasses, moisture convergence is substantially increased, $\Delta(P - E) > 0$, resulting in more latent heat release in the cyclo-
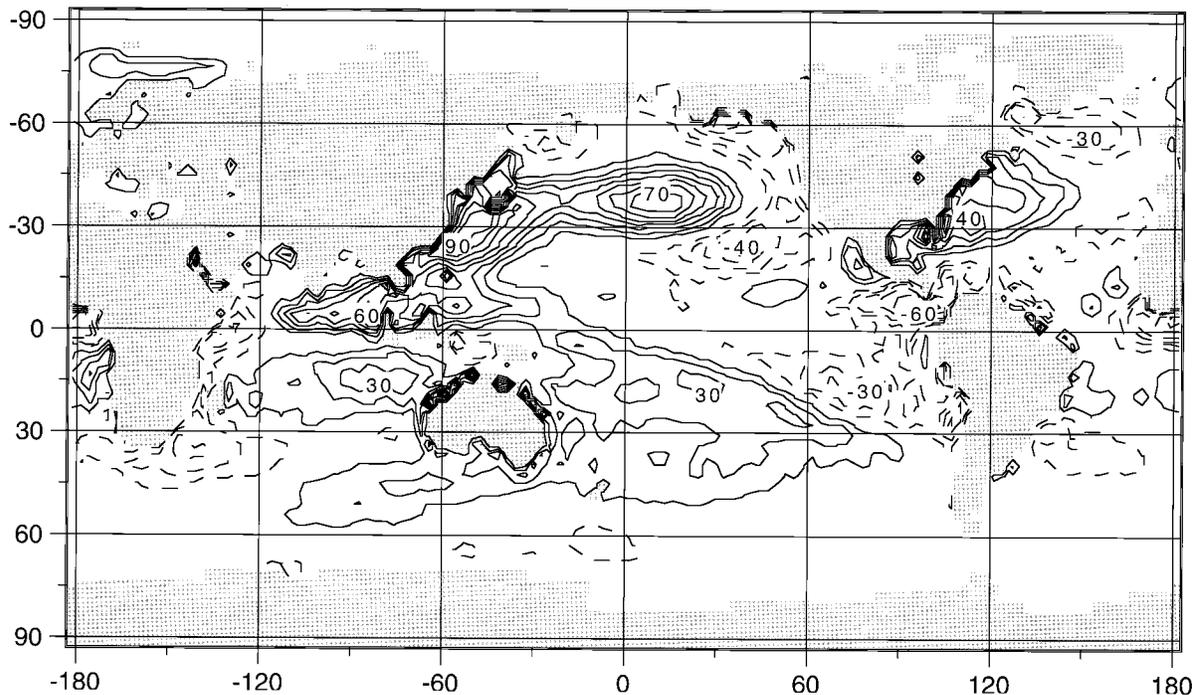
FIG. 5. Annual mean difference in net surface heat flux between the green planet and the desert world. Contour interval is 10 W m^{-2}. Zero difference contour lines are omitted. Grey areas denote land regions. Negative values (dashed contour lines) mean loss of heat from the ocean to the atmosphere.

genesis areas from where the storm tracks start (Fig. 3). These patterns are reflected in the zonally averaged water budget $\Delta(P - E)$, presented on the left panels in Fig. 4. This is also of relevance for the freshwater flux into the oceans.

These results offer a conceptual interpretation: the green planet's enhanced evapotranspiration and precipitable water and the subsequent precipitation is realized by the general circulation through the dynamically relevant systems, that is, the tropical storms and the midlatitude cyclones associated with their rain-bearing fronts. This includes their embedding in the associated larger scale: the ITCZ and the midlatitude storm tracks. Enhanced latent heat release within the ITCZ generates a stronger Hadley cell leading to a substantially warmer upper troposphere in its descending branch over the subtropics. In the storm tracks, the midlatitude cyclones and frontal systems extend the upper-tropospheric warm domain farther poleward due to their contribution to the enhanced precipitation utilizing the larger water content in an atmospheric column. This basic argument requires modification when considering seasonality; in the NH summer, the prevailing continentality makes the midlatitude systems the primary contributor to the observed warm region (described above) that has its core near 50°N, while the SH winter circulation is reduced to the effect of an enhanced Hadley cell. In the SH summer, however, the influence of the continentality is less pro-

nounced in the midlatitudes and more concentrated in the enhanced Hadley cell.

4. Summary and discussion

The approach taken in this note is, basically, a sensitivity analysis simulating the effect of land surface conditions dominated by extremes of homogeneous land vegetation cover on the weather and climate. The extremes of a green planet and a desert world determine globally relevant bounds set by global forests or deserts. The comparison (green planet minus desert world) reveals that the dominant signal is related to changes of the hydrological cycle, which is intensified substantially. The regional changes of the water and heat balance at the surface and in the atmosphere discussed in this note, have potential impact on the ocean and the atmospheric greenhouse.

- The *ocean* is reduced to the prescribed annual cycle of the sea surface temperature, which are associated with the present day climate. Therefore, both green planet and desert world are expected to generate a net heat exchange between ocean and atmosphere that does not balance in the climatological global average. This global imbalance amounts to a loss of 0.6×10^{15} W for the oceans in a desert world and a gain of 1.2×10^{15} W on the green planet. Locally, the sea surface heat exchange occurs predominantly along the west-

ern boundary currents (Fig. 5) with peak differences (green planet minus desert world) of about 100 W m^{-2}. The differences in net surface heat flux over the oceans are explained by the transport of moister and cooler air from the eastern parts of the continents where water recycling is more intense in the green planet. The large magnitude of these values and the freshwater budget discussed above suggests an extension of this analysis utilizing a coupled ocean–atmosphere model.

- The *atmosphere* may be substantially influenced by a green planet. The near-surface cooling (associated with a more stable troposphere) reduces the greenhouse effect, defined by the net terrestrial radiation difference between top and bottom of the atmosphere (Kiehl and Trenberth 1997), $L_{top} - L_{bottom} = 160.3$ and 163.7 W m^{-2} for the green planet or desert world, respectively. The difference shows a remarkable reduction of the greenhouse effect $\Delta(L_{top} - L_{bottom}) = 3.4$ W m^{-2}, which may partially counteract an expected CO_2 induced warming. Note that the carbon cycle dynamics associated with vegetation changes has not been considered in the experiments. However, in a companion paper (Kleidon et al. 1999) the effect on the land surface is discussed.

Here it should be noted that this approach does not consider the known dependencies of vegetation on climate. It is expected that the extremes chosen do not represent sustainable states of biogeography in a natural world. Therefore, these experiments should be considered as a demonstration rather than a precise quantification of the effects of vegetation extremes on global climate. It would be interesting to repeat the study with a fully coupled climate–vegetation model.

REFERENCES

Batjes, N. H., 1996: Development of a world data set of soil water retention properties using pedotransfer rules. *Geoderma,* **71,** 31–52.

Blackmon, M. L., 1976: A climatological study of the 500-mb geopotential height of the Northern Hemisphere. *J. Atmos. Sci.,* **33,** 1607–1623.

Charney, J. G., 1975: Dynamics of deserts and drought in the Sahel. *Quart. J. Roy. Meteor. Soc.,* **101,** 193–202.

Claussen, M., 1998: On multiple solutions of the atmosphere-vegetation system in present day climate. *Global Change Biol.,* **4,** 549–559.

——, U. Lohmann, E. Roeckner, and U. Schulzweida, 1994: A global data set of land surface parameters. Report 135, Max-Planck Institut für Meteorologie, Hamburg, 30 pp. [Available from Max-Planck Institut für Meteorologie, Bundesstr. 55, D 20146 Hamburg, Germany.]

Delworth, T., and S. Manabe, 1988: The influence of potential evaporation on the variabilities of simulated soil wetness and climate. *J. Climate,* **1,** 523–547.

——, and ——, 1989: The influence of soil wetness on near-surface atmospheric variability. *J. Climate,* **2,** 1447–1462.

deNoblet, N., I. C. Prentice, S. Jousaume, D. Texier, A. Botta, and A. Haxeltine, 1996: Possible role of atmosphere–biosphere interactions in triggering the last glaciation. *Geophys. Res. Lett.,* **23** (22), 3191–3194.

Dümenil, L., and E. Todini, 1992: A rainfall-runoff scheme for use in the Hamburg climate model. *Advances in Theoretical Hydrology—A Tribute to James Dooge,* J. P. Kane, Ed., Elsevier, 129–157.

Eltahir, E. A. B., 1998: A soil moisture-rainfall feedback mechanism. 1. Theory and observations. *Water Resour. Res.,* **34,** 765–776.

Foley, J. A., S. Levis, I. C. Prentice, D. Pollard, and S. Thompson, 1998: Coupling dynamic models of climate and vegetation. *Global Change Biol.,* **4,** 561–579.

Henderson-Sellers, A., R. E. Dickinson, T. B. Durbridge, P. J. Kennedy, K. McGuffie, and A. J. Pitman, 1993: Tropical deforestation: Modeling local- to regional-scale climate change. *J. Geophys. Res.,* **98,** 7289–7315.

Kiehl, J. T., and K. E. Trenberth, 1997: Earth's annual global mean energy budget. *Bull. Amer. Meteor. Soc.,* **78,** 197–208.

Kleidon, A., and M. Heimann, 1998a: Optimised rooting depth and its impacts on the simulated climate of an atmospheric general circulation model. *Geophys. Res. Lett.,* **25,** 345–348.

——, and ——, 1998b: Assessing the role of deep rooted vegetation in the climate system with model simulations: Mechanism, comparison to observations and implications for Amazonian deforestation. *Clim. Dyn.,* in press.

——, K. Fraedrich, and M. Heimann, 1999: A green planet versus a desert world: Estimating the maximum effect of vegetation on the land surface climate. *Climate Change,* in press.

Lau, K.-M., J. H. Kim, and Y. Sud, 1996: Intercomparison of hydrologic processes in AMIP GCMs. *Bull. Amer. Meteor. Soc.,* **77,** 2209–2227.

Pielke, R. A., R. Avissar, M. Raupach, A. J. Dolman, X. Zeng, and A. S. Denning, 1998: Interactions between the atmosphere and terrestrial ecosystems: Influence on weather and climate. *Global Change Biol.,* **4,** 461–475.

Roeckner, E., and Coauthors, 1996: The atmospheric general circulation model ECHAM-4: Model description and simulation of present-day climate. Report 218, Max-Planck Institut für Meteorologie, 90 pp. [Available from Max-Planck Institut für Meteorologie, Bundesstr. 55, D-20146 Hamburg, Germany.]

Shukla, J., and Y. Mintz, 1982: The influence of land-surface-evapotranspiration on the earth's climate. *Science,* **247,** 1322–1325.

Stendel, M., and E. Roeckner, 1998: Impacts of horizontal resolution on simulated climate statistics in ECHAM 4. Report 253, Max-Planck Institut für Meteorologie, 57 pp. [Available from Max-Planck Institut für Meteorologie, Bundesstr. 55, D-20146 Hamburg, Germany.]

Sud, Y. C., J. Shukla, and Y. Mintz, 1988: Influence of land-surface roughness on atmospheric circulation and precipitation: A sensitivity study with a general circulation model. *J. Appl. Meteor.,* **27,** 1036–1054.

Vitousek, P. M., H. A. Mooney, J. Lubchenco, and J. M. Melillo, 1997: Human domination of earth's ecosystems. *Science,* **277,** 494–499.

Wild, M., A. Ohmura, H. Gilgen, E. Roeckner, and M. Giorgetta, 1996: Improved representation of surface and atmospheric radiation budgets in the ECHAM4 General Circulation Model. Report 200, Max-Planck Institut für Meteorologie, 32 pp. [Available from Max-Planck Institut für Meteorologie, Bundesstr. 55, D-20146 Hamburg, Germany.]